Synthesis and characterization of peapods and DWCNTs

B. Anis[1], M. Fischer[2], M. Schreck[2], K. Haubner[3], L. Dunsch[3], and C. A. Kuntscher[*,1]

[1] Experimentalphysik 2, Universität Augsburg, 86195 Augsburg, Germany
[2] Experimentalphysik 4, Universität Augsburg, 86195 Augsburg, Germany
[3] Center of Spectroelectrochemistry, IFW Dresden, P.O. Box 270116, 01171 Dresden, Germany

Keywords DWCNTs, infrared spectroscopy, peapods, Raman spectroscopy

[*] Corresponding author: e-mail christine.kuntscher@physik.uni-augsburg.de, Phone: +49 (0)821 598 3315, Fax: +49 (0)821 598 3411

1 Introduction Filling the SWCNTs cavity with fullerene molecules or with an inner tube will alter the electronic and mechanical properties of the nanotubes. It is also possible to fine-tune the nanotubes' properties by changing the filler [1, 2]. Filling the SWCNTs with C_{60} molecules can be discussed in terms of stabilization energy. For small-diameter SWCNTs with diameter $d < 1.2$ nm the interaction between C_{60} and SWCNTs is endothermic and the formed system is unstable [3]; however, for large diameters $\approx$1.22–1.6 nm the interaction is exothermic and the system is stable [3]. At a critical diameter of SWCNTs $d \geq 1.37$ nm the t_{1u} state of C_{60} molecules just start to overlap with the nearly free electron (NFE) state of the SWCNTs, so that the π electron cloud around the nanotube will decrease, that is, the effective tube diameter of the SWCNTs will decrease [3, 4]. As the tube diameter increases above the critical value $d \approx 1.37$ nm, the overlapping between the nanotubes and the C_{60} molecules becomes significant [5]. For thinner SWCNTs with $d \approx 1.22$–1.37 nm, the space between the nanotubes and the C_{60} molecules is not sufficient enough to generate the NFE state and hence the effective tube diameters will increase due to the filling [4, 6]. According to the results from optical measurements, for smaller diameter SWCNTs with $d = 1.22$–1.37 nm, the average tubes' diameter increases with C_{60} molecules filling and leads to a red shift in the absorptions bands, in contrast to larger diameter tubes ($d = 1.4$–1.6 nm), where a blue shift is found [4, 6].

Raman measurements on C_{60}@SWCNT peapods show a blue shift of the radial breathing modes (RBMs) compared to the empty SWCNTs with average tube diameters $\approx$1.37 nm [5, 7] and a red shift in the case of SWCNTs with average tube diameters $\approx$1.4–1.6 nm [5, 8, 9]. The hardening of the RBMs for the small tube diameters was attributed to the hindrance of the radial motion of the tubes with the C_{60} molecules filling [5, 7]. In contrast, the red shift of the RBMs in the case of thicker tubes was attributed to the C–C bond softening of the SWCNTs due to the charge transfer between the SWCNTs and C_{60} molecules [5, 8, 9]. Scanning tunneling microscopy found a modification of the total electronic structure of the SWCNTs after filling with C_{60} molecules [10, 11].

Here, we report the preparation of high-yield of SWCNTs encapsulating C_{60} fullerene molecules and also the preparation of DWCNTs derived from the C_{60}@SWCNT peapods. The prepared samples were characterized by Raman and optical spectroscopy. The effects of the interaction between the fillers (fullerene molecules, inner tube) and the SWCNT on the electronic and vibrational properties are discussed.

2 Experimental Bundled SWCNTs were purchased from Carbon Solutions Inc. (Type P2, average diameter 1.4 nm). C_{60}-fullerene with purity 99.98% was purchased from Term USA. To obtain peapods with a high filling ratio, the gas phase method was used [12]. The typical preparation method is the following: the caps of the SWCNTs were opened by heating the sample in furnace at 575 °C for 30 min. Weighted amounts of SWCNTs and C_{60} were degassed under dynamic vacuum at 200 °C for 24 h, after that both samples were sealed in quartz tube under vacuum and heated at 750 °C for 5 days continuously. The non-reacted fullerene molecules were removed by heating the sample at 700 °C under dynamic vacuum for 3 h. The prepared peapods were then transformed to DWCNTs by tempering the purified sample at 1250 °C for 24 h under dynamic vacuum and subsequently cooling the furnace to room temperature. Free-standing films from SWCNTs and DWCNTs for IR spectroscopy measurements were prepared from Triton X-100 suspension [13].

Raman spectra were recorded at room temperature with a triple Raman spectrometer T64000 (Horiba Jobin Yvon), interfaced to an Olympus BX-40 microscope (100× objective) and the 488 nm line of an argon ion laser. The laser power impinging on the sample was 0.1 mW.

Transmission data were obtained at ambient conditions in the frequency range 2500–20,000 cm^{-1} using a Bruker IFS 66v/S Fourier transform infrared spectrometer in combination with an infrared microscope (Bruker IR Scope II) with a 15× magnification objective. The intensity $I_{sample}(\omega)$ of the radiation transmitted through the free-standing film and, as reference, the intensity $I_{ref}(\omega)$ of the radiation transmitted through air was measured. From $I_{sample}(\omega)$ and $I_{ref}(\omega)$ the transmittance and absorbance spectra were calculated according to $T(\omega) = I_{sample}(\omega)/I_{ref}(\omega)$ and $A(\omega) = -\log_{10} T(\omega)$, respectively.

3 Results and discussion The RBMs of the SWCNTs, peapods, and the outer tubes of the DWCNTs appear in the low-frequency range (140–200 cm^{-1}) of the Raman spectra, as depicted in Fig. 1. The peaks are located between 160 and 192 cm^{-1}. The spectra were fitted with Lorentzian functions, in order to specify the various contributions, and the so-obtained peak positions are given in the spectra. According to theoretical calculations the diameter d of the tubes is related to the frequency ω_r according to the relation $d = A/(\omega_r)$, where A is a constant. Hereby, the small effect of the tube–tube interaction is neglected. In the following we assume a mean value $A \approx 234$ [14]. In this case the uncertainty in the diameter calculations is around 5% [14]. From the above relation the calculated values for the SWCNTs diameters are ~1.45–1.23 nm, in agreement with the average tube diameter (~1.4 nm).

One notices that the RBMs of the peapods are shifted by a small amount ~2 cm^{-1} towards higher frequencies. Since the average tube diameters is 1.4 nm and the C_{60} molecule diameter is 0.71 nm [15], the difference in the mean diameter

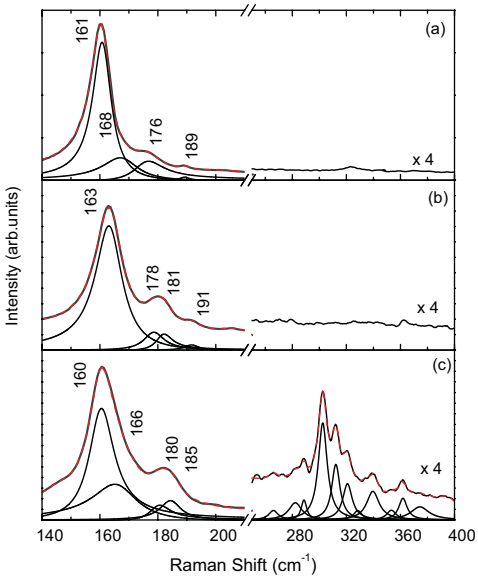

Figure 1 (online color at: www.pss-b.com) Raman spectra of the RBMs for (a) SWCNTs, (b) peapods, and (c) DWCNTs. Modes in the range 270–400 cm^{-1} in (c) correspond to the RBMs of the inner tubes. Raman spectra in the range 270–400 cm^{-1} were multiplied by a factor of 4. The red-dashed line is a fit to the data with Lorentzian functions.

between the two species is ≈0.7 nm. This value is consistent with the π electron cloud thickness ~0.34 nm around the SWCNTs wall, suggesting that the C_{60} molecules are tightly nested inside the nanotubes. Therefore, filling of 1.4 nm SWCNTs with C_{60} will hinder the radial motion of the nanotubes, and hence shift the RBM modes to higher frequencies [5, 7]. On the other hand, the RBMs in the DWCNTs are shifted towards lower frequencies by ~2–4 cm^{-1}. This downshift can be attributed to the outer tubes fattening with the long heat treatments (1250 °C and 24 h) via several Stone–Wales transformation on the SWCNTs surface [16].

In the frequency range 250–400 cm^{-1} no Raman features are observed for the SWCNTs and peapods. In contrast, in the case of DWCNTs several new peaks with quite low intensity are found. These new peaks are associated with the smaller E_{22}^{S} semiconducting secondary tubes with ~0.7 nm inside the DWCNTs [8, 14]. The 488 nm excitation is unsuitable for secondary tubes resonant enhancement, and therefore the quite low intensity is expected [14]. According to $d = A/(\omega_r)$ (see above), the values for the inner tubes' diameters amount to 0.65–0.85 nm. These values are higher than the diameter of the C_{60} molecules (0.71 nm). This difference could be attributed to the tubes fattening due to long heat treatment [16].

Figure 2 shows the tangential mode region for (a) SWCNTs, (b) peapods, and (c) DWCNTs. In the frequency range 1400–1500 cm^{-1} no clear Raman features are observed for the SWCNTs and DWCNTs. In contrast, in the case of peapods, we can see the Raman-active mode $A_g(2)$ of the C_{60} molecules at 1465 cm^{-1}. The average

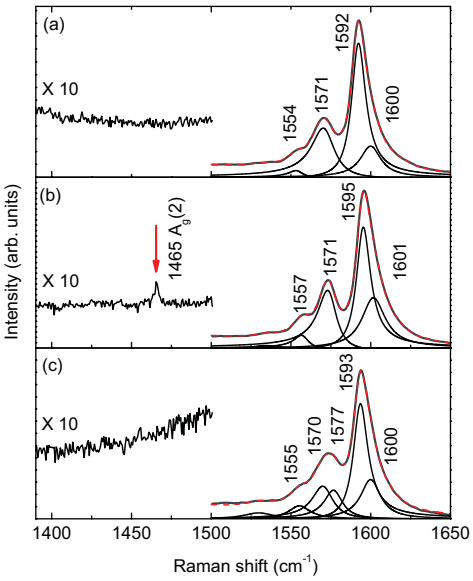

Figure 2 (online color at: www.pss-b.com) Raman spectra of the tangential mode for (a) SWCNTs, (b) peapods, and (c) DWCNTs. The mode at 1465 cm^{-1} in (b) corresponds to the $A_g(2)$ of the C_{60} molecules. Raman spectra in the range 1400–1500 cm^{-1} were multiplied by a factor of 10. The red-dashed line is a fit to the data with Lorentzian functions.

integrated intensity ratio $A_g(2)$/G-mode $= 4 \times 10^{-3}$ suggests that the C_{60} molecules are encapsulated inside the nanotubes and indicates a high filling ratio of the peapods [17, 18]. The filling ratio of the C_{60} peapod and DWCNT samples was determined by HRTEM (not shown) to be $\geq$95% [19]. In the frequency range 1500–1650 cm^{-1} the broad tangential G modes are observed for all studied samples. For the SWCNTs the mode centered at 1593 cm^{-1} is related to the G^+ peak [20, 21]. The two lower-frequency bands appeared at 1554 and 1571 cm^{-1} are related to the G^- peak. The extra peak around 1600 cm^{-1} originates from the E_1^{TO} (M, S) modes [20, 21]. For the peapods (Fig. 2b) the three components of the G mode are blue shifted. This could be attributed to the radial overlapping between the π states of SWCNTs and C_{60} molecules which causes a reduction on the C–C bond length [22]. In the case of DWCNTs (Fig. 2c), we can observe a new peak centered at 1577 cm^{-1}, which can be assigned to the small secondary semiconducting tubes with a mean diameter of 0.8 nm [14].

Figure 3 shows the background-subtracted absorbance spectra of (a) SWCNTs, (b) peapods, and (c) DWCNTs free-standing films. The absorption bands S_{ii} and M_{ii} correspond to the ith optical transition in the semiconducting and metallic SWCNTs, respectively. The inset of Fig. 3 depicts the raw absorbance spectrum of the free-standing SWCNTs and the absorbance spectrum after the background subtraction. The broad background is due to the π–π^* absorption centered at around 5 eV and follows an approximately linear behavior. The fine structure of the absorption bands is due to the diameter distributions. The absorption bands were fitted with Lorentzian oscillators and the contributions are

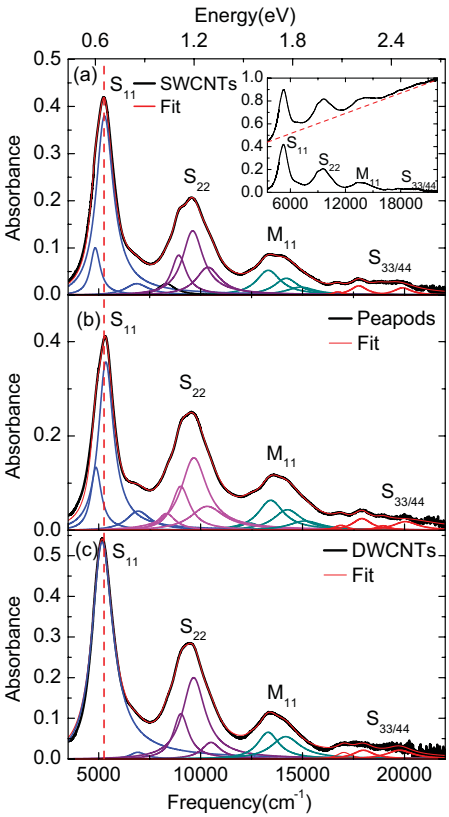

Figure 3 (online color at: www.pss-b.com) Background-subtracted absorbance spectra of (a) SWCNTs, (b) peapods, and (c) DWCNTs together with the fit of the absorption bands using Lorentzian oscillators. The vertical, dashed line marks the position of the S_{11} band in SWCNTs. Inset: absorbance spectrum for the SWCNTs film together with the linear background (dashed red line) and the absorbance spectrum after background subtraction.

listed in Table 1. According to Fig. 3, in peapods all the Lorentzian contributions are slightly shifted to higher energies, and in DWCNTs all contributions are slightly shifted to lower energies compared to the corresponding features in SWCNTs (see Table 1). In the case of peapods, a hybridization between the NFE state of the SWCNTs and the t_{1u} state of the C_{60} is expected, since the average tube diameter is nearly equal to the critical value at which the

Table 1 Peak positions in cm^{-1} of the Lorentz contributions of the S_{11}, S_{22}, M_{11}, and $S_{33/44}$ for SWCNTs, peapods, and DWCNTs.

	S_{11}	S_{22}	M_{11}	$S_{33/44}$
SWCNTs	4800	8960	13,300	17,763
	5255	9610	14,180	18,873
	6920	10,330	15,098	19,909
peapods	4866	9020	13,440	16,875
	5350	9670	14,260	17,911
	6940	10,340	15,120	18,947
DWCNTs	–	8930	13,270	17,700
	5185	9580	14,100	18,780
	6870	10,300	–	19,835

hybridization starts. In this case the hybridization is expected to reduce the effective tube diameter, and hence the optical absorption bands are blue-shifted [4, 22]. In case of the DWCNTs, due to the fattening of the tubes with long heat treatment the effective tube diameters will increase [16], and hence the absorption bands will be shifted to lower energies according to the Kataura plot [23].

4 Conclusions We have prepared high-yield C_{60}-peapods and DWCNTs and compared their vibrational and electronic properties to SWCNTs. In the case of peapods the C_{60} molecules hinder the radial motion of the SWCNTs, causing a shift of the RBMs to higher frequencies. In DWCNTs the downshift of the RBMs demonstrate a diameter increase compared to SWCNTs due to tube fattening. The inner tubes' diameters in the DWCNTs range from 0.65 to 0.85 nm, as derived from the RBM frequencies. Filling the tubes with C_{60} molecules shifts the G mode to higher energies due to the shorting of the C–C bonds of the SWCNTs. In the case of DWCNTs the new mode centered at 1577 cm^{-1} is due the small secondary semiconducting tubes with mean diameter of 0.8 nm. In comparison with SWCNTs all the optical transitions shift to higher energies in the case of peapods due to average tube diameter reduction, whereas they shift to lower energies in the case of DWCNTs due to tube fattening. These findings reflect that in the tube diameter range $\sim$1.37–1.4 nm, the C_{60} molecules play two roles: (i) hindrance of the radial motion of SWCNTs and shifting the RMBs to higher frequencies and (ii) overlapping with the NFE states of the SWCNTs causing a reduction of the π electron cloud around the nanotube.

Acknowledgements This work is financially supported by the DFG, the DAAD, and the Egyptian Government.

References

[1] F. Simon, H. Kuzmany, H. Rauf, T. Pichler, J. Bernardi, H. Peterlik, L. Korecz, F. Fülöp, and A. Jánossy, Chem. Phys. Lett. **383**, 362 (2004).
[2] T. Shimada, Y. Ohno, K. Suenaga, T. Okazaki, S. Kishimoto, T. Mizutani, R. Taniguchi, H. Kato, B. Cao, T. Sugai, and H. Shinohara, Jpn. J. Appl. Phys. **44**, 469 (2005).
[3] A. Rochefort, Phys. Rev. B **67**, 115401 (2003).
[4] A. G. Ryabenko, N. A. Kiselev, J. L. Hutchison, T. N. Moroz, S. S. Bukalov, L. A. Mikhalitsyn, R. O. Loutfy, and A. P. Moravsky, Carbon **45**, 1492 (2007).
[5] S. Okada, Chem. Phys. Lett. **438**, 59 (2007).
[6] X. Liu, T. Pichler, M. Knupfer, M. S. Golden, J. Fink, H. Kataura, Y. Achiba, K. Hirahara, and S. Iijima, Phys. Rev. B **65**, 045419 (2002).
[7] S.-K. Joung, T. Okazaki, S. Okadac, and S. Iijimaa, Phys. Chem. Chem. Phys. **12**, 8118 (2010).
[8] S. Bandow, M. Takizawa, K. Hirahara, M. Yudasaka, and S. Iijima, Chem. Phys. Lett. **337**, 48 (2001).
[9] S. Bandow, M. Takizawa, H. Kato, T. Okazaki, H. Shinohara, and S. Iijima, Chem. Phys. Lett. **347**, 23 (2001).
[10] D. J. Hornbaker, S.-J. Kahng, S. Misra, B. W. Smith, A. T. Johnson, E. J. Mele, D. E. Luzzi, and A. Yazdani, Science **295**, 828 (2002).
[11] C. L. Kane, E. J. Mele, A. T. Johnson, D. E. Luzzi, B. W. Smith, D. J. Hornbaker, and A. Yazdani, Phys. Rev. B **66**, 235423 (2002).
[12] K. Hirahara, K. Suenaga, S. Bandow, H. Kato, T. Okazaki, H. Shinohara, and S. Iijima, Phys. Rev. Lett. **85**, 5384 (2000).
[13] Z. Wu, Z. Chen, X. Du, J. M. Logan, J. Sippel, M. Nikolou, K. Kamaras, J. R. Reynolds, D. B. Tanner, A. F. Hebard, and A. G. Rinzler, Science **305**, 1273 (2004).
[14] S. Bandow, G. Chen, G. U. Sumanasekera, R. Gupta, M. Yudasaka, S. Iijima, and P. C. Eklund, Phys. Rev. B **66**, 075416 (2002).
[15] M. S. Dresselhaus, G. Dresselhaus, and P. C. Eklund, Science of Fullerenes and Carbon Nanotubes (Academic Press, San Diego, 1996), p. 63.
[16] F. Ding, Z. Xu, B. I. Yakobson, R. J. Young, I. A. Kinloch, S. Cui, L. Deng, P. Puech, and M. Monthioux, Phys. Rev. B **82**, 041403 (2010).
[17] H. Kuzmany, R. Pfeiffer, Ch. Kramberger, T. Pichler, X. Liu, M. Knupfer, J. Fink, H. Kataura, Y. Achiba, B. W. Smith, and D. E. Luzzi, Appl. Phys. A **76**, 449 (2003).
[18] H. Kuzmany, R. Pfeiffer, F. Simon, Ch. Kramberger, M. Hulman, and P. Costa, Fullerenes Nanotubes Carbon Nanostruct. **13**(S1), 179–188 (2005).
[19] B. Anis, K. Haubner, F. Börrnert, L. Dunsch, M. H. Rümmeli, and C. A. Kuntscher, Phys. Rev. B (submitted).
[20] V. N. Popov and P. Lambin, Phys. Rev. B **73**, 165425 (2006).
[21] H. Rauf, T. Pichler, R. Pfeiffer, F. Simon, H. Kuzmany, and V. N. Popov, Phys. Rev. B **74**, 235419 (2006).
[22] S. Okubo, T. Okazaki, N. Kishi, S.-K. Joung, T. Nakanishi, S. Okada, and S. Iijima, J. Phys. Chem. C **113**, 571 (2009).
[23] H. Kataura, Y. Kumazawa, Y. Maniwa, I. Umezu, S. Suzui, Y. Ohtsuka, and Y. Achiba, Synth. Met. **103**, 255 (2009).